



Source point isolation boundary element method for solving general anisotropic potential and elastic problems with varying material properties

Xiao-Wei Gao

State Key Laboratory of Structural Analysis for Industrial Equipment, Dalian University of Technology, Dalian 116024, PR China

ARTICLE INFO

Article history:

Received 1 February 2010
Accepted 30 June 2010

Keywords:

Boundary element method
Source point isolation technique
Anisotropic potential problem
Anisotropic elasticity
Varying material property

ABSTRACT

This paper presents a new robust boundary element method, based on a source point isolation technique, for solving general anisotropic potential and elastic problems with varying coefficients. Different types of fundamental solutions can be used to derive the basic integral equations for specific anisotropic problems, although fundamental solutions corresponding to isotropic problems are recommended and adopted in the paper. The use of isotropic fundamental solutions for anisotropic and/or varying material property problems results in domain integrals in the basic integral equations. The radial integration method is employed to transform the domain integrals into boundary integrals, resulting in a pure boundary element analysis algorithm that does not need any internal cells. Numerical examples for 2D and 3D potential and elastic problems are given to demonstrate the correctness and robustness of the proposed method.

© 2010 Elsevier Ltd. All rights reserved.

1. Introduction

Although the boundary element method (BEM) has been successfully established and applied in engineering as an effective and convenient numerical tool for finding the solution to a wide class of boundary value problems [1], its application to general anisotropic and non-linear problems is not as effective as to linear isotropic problems. The main reason is that the anisotropy of a material increases the number of material properties, and hence makes the fundamental solutions either too complex or unavailable in a closed form [2–4]. To obtain fundamental solutions for general anisotropic solids, Mura [5] investigated line-integral representations of the three-dimensional Green's function in a full-space medium. Based on complex potential theory, Lekhnitskii [6] and Sollero [7] gave anisotropic fundamental solutions based on finding roots of a characteristic fourth degree polynomial equation [8]. Using Lekhnitskii's fundamental solutions, Shiah and Tan solved 2D anisotropic elasticity problems with body forces [9], in which volume integrals involving the body forces are transformed into surface integrals by applying a differentiation technique before doing an analytical transformation. Wang [10] in 1997 derived explicit expressions for three-dimensional elastostatic Green's displacement in general anisotropic solids. In Wang's work, the numerical solution of a polynomial of sixth order is required in order to obtain the entire Green's function. Wang's work is purely theoretical. Later, Tonon et al. [11] applied Wang's work to a boundary element

implementation. Also in 1997 [12], Ting and Lee derived explicit expressions for the anisotropic Green's functions in terms of the Stroh eigenvalues [13]. For multi-medium problems, Fares and Li [14] constructed the Green's functions for multilayered media using a general image method. By utilizing an inverse Fourier transform in polar coordinates and combining with Mindlin's superposition method, Pan and Yuan [15] derived an expression of Green's functions for anisotropic half-space and bimaterial problems.

The works described above can result in pure boundary-only integral equations for anisotropic problems with constant material parameters. The drawback of these works is that evaluating a line integral or solving an eigenvalue equation set is cumbersome and often time-consuming. For some problems, deriving a closed form of fundamental solutions, especially stress fundamental solutions, is either very difficult in itself or requires complicated coding of the resulting expression. Besides, for multi-medium problems, a closed form of the fundamental solutions may be unavailable and numerical integration of a line integral may be necessary. This may result in the dependence of Green's functions on material properties [15]. On the other hand, obtaining fundamental solutions for generating pure boundary integral equations may never be possible for anisotropic problems involving varying material properties as occurs in functionally graded material problems (FGMs) [16]. Therefore, a new method needs to be exploited for solving general anisotropic problems associated with advanced materials.

In a different manner, Schlar and Partridge [17] proposed an approach to solve anisotropic problems based on the use of the fundamental solutions, for a homogeneous material, which leads

E-mail address: xwgao@dlut.edu.cn

to a boundary-domain integral equation due to the residuals between the actual and the isotropic quantities. In this approach, to achieve a boundary-only BEM algorithm, the dual reciprocity method (DRM) [18] is used to take the relevant domain integral to the boundary. The main advantage of this approach [17] is that the anisotropic fundamental solution is avoided and, therefore, it is easier to apply in solving different types of anisotropic problems. In a similar way, Chen et al. [19,20] converted the resulting domain integrals to the boundary based on the method of fundamental solutions and DRM. The work in [17] is only suitable for constant material problems, and, since it relies on the use of DRM to convert domain integrals to the boundary, certain amounts of internal points may be required to ensure a satisfactory computational accuracy.

In this paper, a new and simple BEM, named Source-point Isolation Boundary Element Method (SIBEM), is proposed for solving general anisotropic potential and elastic problems. The method is based on a source-point isolation technique and allows for material properties to be variable. Different types of fundamental solutions can be used in the derived integral equations. For constant material property problems, if the fundamental solutions used are the ones of the corresponding problem, pure boundary integral representation can be preserved. However, as used in this paper, if the fundamental solution of the homogeneous material is used for anisotropic problems or for problems, in which material properties are not constant, the resulting integral equation includes domain integrals. In this case, the radial integration method (RIM) [21,22] is adopted to transform the domain integrals into boundary integrals. For large gradient potential/elastic problems, some internal points may be needed to improve the accuracy. However, for general engineering problems, few or even no internal points are needed to obtain a satisfactory result [16]. While both RIM and DRM need to use RBFs to approximate the unknowns included in the domain integrals, it should be pointed out that DRM transforms domain integrals to the boundary by employing particular solutions derived from the differential operator of the problem, whereas an RIM can transform any domain integrals to the boundary based on purely mathematical treatments without needing any particular solutions [23,24]. In numerical examples, 2D and 3D anisotropic potential and elastic problems are given to demonstrate the correctness and robustness of the proposed method. Also, the challenging problem of the honeycomb sandwich structure is particularly introduced to show the ability of the proposed techniques to solve complex 3D geometry problems with strong contrasts in material properties.

2. Boundary-domain integral equations for general potential problems based on source point isolation technique

2.1. Formulations for general potential problems

The governing equation for general potential problems can be expressed as [25]

$$\frac{\partial}{\partial x_i} \left(k_{ij} \frac{\partial T}{\partial x_j} \right) + Q = 0 \tag{1}$$

where k_{ij} and Q are the material property tensor and source terms, respectively, and T denotes the potential. They may all be functions of spatial coordinates for non-homogeneous problems or functions of field variables for non-linear problems. It is noted that the material property tensor is symmetric, i.e., $k_{ij} = k_{ji}$. The repeated subscripts in Eq. (1) represent summation over the ranges of their values. Using a weight function G to multiply both sides of Eq. (1) and integrating over the whole domain Ω , the

following weak form can be written.

$$\int_{\Omega} G \frac{\partial}{\partial x_i} \left(k_{ij} \frac{\partial T}{\partial x_j} \right) d\Omega + \int_{\Omega} G Q d\Omega = 0 \tag{2}$$

The first integral can be manipulated as follows:

$$\begin{aligned} \int_{\Omega} G \frac{\partial}{\partial x_i} \left(k_{ij} \frac{\partial T}{\partial x_j} \right) d\Omega &= \int_{\Gamma} G k_{ij} \frac{\partial T}{\partial x_j} n_i d\Gamma - \int_{\Omega} \frac{\partial G}{\partial x_i} k_{ij} \frac{\partial T}{\partial x_j} d\Omega \\ &= - \int_{\Gamma} G q d\Gamma - \int_{\Gamma} q^* T d\Gamma + \int_{\Omega} \frac{\partial}{\partial x_j} \left(k_{ij} \frac{\partial G}{\partial x_i} \right) T d\Omega \\ &= - \int_{\Gamma} G q d\Gamma - \int_{\Gamma} q^* T d\Gamma + I_{\Omega} \end{aligned} \tag{3}$$

where

$$\begin{aligned} q &= -k_{ij} \frac{\partial T}{\partial x_j} n_i \\ q^* &= \frac{\partial G}{\partial x_i} k_{ij} n_j \end{aligned} \tag{4}$$

$$I_{\Omega} = \int_{\Omega} \frac{\partial}{\partial x_j} \left(k_{ij} \frac{\partial G}{\partial x_i} \right) T d\Omega \tag{5}$$

in which Γ denotes the boundary of the domain Ω , n_i is the i -th component of the outward normal vector to Γ , and q is the flux. It is noted that the domain integral in Eq. (5) may be strongly singular (depending on the choice of G) and, therefore, a different integral symbol is used to denote this.

We assume that the weight function G is a fundamental solution of either isotropic or anisotropic problems. Usually, it is a function of the distance r between the source point p and field point q [25,26]. When $r \rightarrow 0$, G may be singular and, therefore, an infinitesimal circular domain Ω_{ε} centered at the source point p with radius ε can be isolated from Ω (Fig. 1).

The last term in Eq. (3) now can be written as

$$\begin{aligned} I_{\Omega} &= \int_{\Omega} \frac{\partial}{\partial x_j} \left(k_{ij} \frac{\partial G}{\partial x_i} \right) T d\Omega = \lim_{\varepsilon \rightarrow 0} \int_{\Omega_{\varepsilon}} \frac{\partial}{\partial x_j} \left(k_{ij} \frac{\partial G}{\partial x_i} \right) T d\Omega \\ &\quad + \lim_{\varepsilon \rightarrow 0} \int_{\Omega - \Omega_{\varepsilon}} \frac{\partial}{\partial x_j} \left(k_{ij} \frac{\partial G}{\partial x_i} \right) T d\Omega \\ &= T(p) \lim_{\varepsilon \rightarrow 0} \int_{\Omega_{\varepsilon}} \frac{\partial}{\partial x_j} \left(k_{ij} \frac{\partial G}{\partial x_i} \right) d\Omega + \int_{\Omega} \frac{\partial}{\partial x_j} \left(k_{ij} \frac{\partial G}{\partial x_i} \right) T d\Omega \\ &= -k(p)T(p) + \int_{\Omega} VT d\Omega \end{aligned} \tag{6}$$

where

$$k(p) = -\lim_{\varepsilon \rightarrow 0} \int_{\Omega_{\varepsilon}} \frac{\partial}{\partial x_i} \left(k_{ij} \frac{\partial G}{\partial x_j} \right) d\Omega = -\lim_{\varepsilon \rightarrow 0} \int_{\Gamma_{\varepsilon}} k_{ij} \frac{\partial G}{\partial x_j} n_i d\Gamma$$

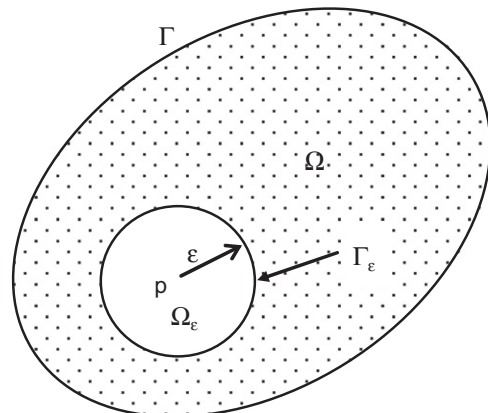


Fig. 1. An infinitesimal domain Ω_{ε} isolated from Ω .

$$= -k_{ij}(p)\lim_{\varepsilon \rightarrow 0} \int_{\Gamma_\varepsilon} \frac{\partial G}{\partial x_i} n_j d\Gamma \quad (7)$$

$$V = \frac{\partial}{\partial x_i} \left(k_{ij} \frac{\partial G}{\partial x_j} \right) = \frac{\partial k_{ij}}{\partial x_i} \frac{\partial G}{\partial x_j} + k_{ij} \frac{\partial^2 G}{\partial x_i \partial x_j} \quad (8)$$

It is noted that the last domain integral in Eq. (6) is interpreted in the Cauchy principal value sense. Substituting Eq. (6) into Eq. (3) and the result into Eq. (2) yields

$$kT + \int_{\Gamma} q^* T d\Gamma = - \int_{\Gamma} Gq d\Gamma + \int_{\Omega} VT d\Omega + \int_{\Omega} GQ d\Omega \quad (9)$$

Eq. (9) is a boundary-domain integral equation valid for isotropic, anisotropic, linear and nonlinear potential problems. The weight function G can be any type of function. If G is a regular function, the coefficient k as determined by Eq. (7) will be zero since the radius $\varepsilon \rightarrow 0$. If G is chosen as the Green's function [2–14] which is weakly singular when source point p approaches the field point under integration, k has a finite value. Finally, if G is chosen as a higher-order singular function than the Green's function, k is infinite and, therefore, this type of G does not make sense. Once the weight function G and material coefficient tensor k_{ij} are given, all coefficients and kernel functions in Eq. (9) are known, and the unknown quantities in it can be solved using the standard BEM discretization procedure [26–28].

It is noted that although Eq. (9) is derived for an internal source point p , it can also be used for boundary nodes since it is actually not necessary to directly compute the coefficient k using Eq. (7). This is based on the fact that the contribution of k to the final system of equations is in the diagonal term, which can be determined using a more efficient way, i.e., the “rigid body motion condition” [27,28].

2.2. Using isotropic fundamental solutions for general anisotropic potential problems

In principle, the weight function G can be any function. However, the simplest way is to choose G as the Green's function for isotropic potential problems, i.e.,

$$G = \begin{cases} \frac{-1}{2\pi} \ln(r) & 2D \\ \frac{1}{4\pi r} & 3D \end{cases} \quad (10)$$

where r is the distance between the source point p and field point q . The derivatives of G with respect to field point coordinates can be derived from Eq. (10) and expressions derived for derivatives of the distance r [28], which can be expressed as

$$\frac{\partial G}{\partial x_i} = \frac{-1}{2\pi\alpha r^\alpha} r_{,i} \quad (11)$$

$$\frac{\partial^2 G}{\partial x_i \partial x_j} = \frac{-1}{2\pi\alpha r^\beta} (\delta_{ij} - \beta r_{,i} r_{,j}) \quad (12)$$

where $r_{,i} = \partial r / \partial x_i$, $\beta=2$ for 2D and $\beta=3$ for 3D problems, and $\alpha=\beta-1$. Since Γ_ε is a circle (2D) or a sphere (3D), we have $n_{,j} = r_{,j}$. Thus, from Eq. (7), it follows that

$$k = \frac{k_{ij}}{2\pi\alpha} \int_{\Gamma_\varepsilon} \frac{r_{,i} n_j}{r^\alpha} d\Gamma = \frac{k_{ij}}{2\pi\alpha} \int_{\Gamma_\varepsilon} \frac{r_{,i} r_{,j}}{r^\alpha} d\Gamma \quad (13)$$

For an internal point, using relationship [21,28]

$$\int_{\Gamma_\varepsilon} \frac{r_{,i} r_{,j}}{r^\alpha} d\Gamma = \begin{cases} \pi \delta_{ij} & 2D \\ \frac{4\pi}{3} \delta_{ij} & 3D \end{cases} \quad (14)$$

Eq. (13) can be integrated as

$$k = k_{ii} / \beta \quad (15)$$

It can be seen that k is the average value of the diagonal term of k_{ij} . This is helpful for understanding the coefficient k in Eq. (9). It is also noted that if the problem solved is isotropic, the last term in Eq. (8) is zero and Eq. (9) is reduced to the result in [26].

3. Boundary-domain integral equations for general elasticity problems based on source point isolation technique

3.1. Formulations for general elasticity problems

The elastic constitutive relationship can be expressed as [27,28]

$$\sigma_{kl} = D_{klrs} \varepsilon_{rs} = D_{klrs} u_{r,s} \quad (16)$$

where σ_{kl} denotes the stress tensor, D_{klrs} is the constitutive tensor, $\varepsilon_{rs} = (u_{r,s} + u_{s,r})/2$ is the strain tensor and u_r is the displacement vector. D_{klrs} may be functions of spatial coordinates for non-homogeneous problems or functions of stresses or strains for non-linear problems. It is noted that D_{klrs} is a symmetric tensor, i.e., $D_{klrs} = D_{rskl} = D_{lkrs} = D_{klsr}$. The comma, 'in the place of subscript represents the spatial derivative, i.e., $u_{r,s} = \partial u_r / \partial x_s$. The stress equilibrium equation with the body force b_k can be expressed as

$$\sigma_{kl,l} + b_k = 0 \quad (17)$$

Using weight functions U_{ik} , the weak form of Eq. (17) can be written as

$$\int_{\Omega} U_{ik} \sigma_{kl,l} d\Omega + \int_{\Omega} U_{ik} b_k d\Omega = 0 \quad (18)$$

The first integral of the above equation can be manipulated as follows

$$\begin{aligned} \int_{\Omega} U_{ik} \sigma_{kl,l} d\Omega &= \int_{\Gamma} U_{ik} \sigma_{kl} n_l d\Gamma - \int_{\Omega} U_{ik,l} \sigma_{kl} d\Omega \\ &= \int_{\Gamma} U_{ik} t_k d\Gamma - \int_{\Omega} U_{ik,l} D_{klrs} u_{r,s} d\Omega \\ &= \int_{\Gamma} U_{ik} t_k d\Gamma - \int_{\Gamma} U_{ik,l} D_{kljs} n_s u_j d\Gamma + \int_{\Omega}^- (U_{ik,l} D_{klrs})_{,s} u_r d\Omega \\ &= \int_{\Gamma} U_{ij} t_j d\Gamma - \int_{\Gamma} T_{ij} u_j d\Gamma + \int_{\Omega}^- (U_{ik,l} D_{kljs})_{,s} u_j d\Omega \end{aligned} \quad (19)$$

where

$$T_{ij} = U_{ik,l} D_{kljs} n_s \quad (20)$$

$$t_k = \sigma_{kl} n_l \quad (21)$$

Similar to the treatment in Section 2, an infinitesimal circular domain Ω_ε is isolated from Ω (Fig. 1). Thus, the last term in Eq. (19) can be expressed as

$$\int_{\Omega}^- (U_{ik,l} D_{kljs})_{,s} u_j d\Omega = -\mu_{ij}(p) u_j(p) + \int_{\Omega} V_{ij} u_j d\Omega \quad (22)$$

where

$$\mu_{ij} = -\lim_{\varepsilon \rightarrow 0} \int_{\Gamma_\varepsilon} U_{ik,l} D_{kljs} n_s d\Gamma = -D_{kljs} \lim_{\varepsilon \rightarrow 0} \int_{\Gamma_\varepsilon} U_{ik,l} n_s d\Gamma \quad (23)$$

$$V_{ij} = (U_{ik,l} D_{kljs})_{,s} = U_{ik,l} D_{kljs,s} + U_{ik,ls} D_{kljs} \quad (24)$$

Substituting Eq. (22) into Eq. (19) and the result into Eq. (18), the following boundary-domain integral equation can be obtained.

$$\mu_{ij} u_j + \int_{\Gamma} T_{ij} u_j d\Gamma = \int_{\Gamma} U_{ij} t_j d\Gamma + \int_{\Omega} V_{ij} u_j d\Omega + \int_{\Omega} U_{ij} b_j d\Omega \quad (25)$$

Eq. (25) is a boundary-domain integral equation, which can be used for isotropic, anisotropic, linear, and nonlinear problems. For nonlinear problems, the effect of nonlinearity is embodied in the derivatives of the constitutive tensor D_{klrs} with respect to spatial coordinates (see Eq. (24)). For detailed procedures for solving nonlinear problems, the reader is referred to the treatment of damage mechanics problems in Ref. [29]. The weight function U_{ij} can be any type of function. All discussions for G and Eq. (9) in Section 2 can be applied to U_{ij} and Eq. (25). Once the forms of U_{ij} and D_{klrs} are given, the coefficient μ_{ij} and all kernel functions in Eq. (25) are known, and the unknown quantities included in Eq. (25) can be solved using the standard BEM discretization procedure [27,28]. It is noted that μ_{ij} actually does not need to be computed for the displacement integral Eq. (25), since it can be determined indirectly using the “rigid body motion condition” [27,28].

3.2. Using Kelvin’s fundamental solutions for general anisotropic elasticity problems

In the following, the weight function U_{ij} is taken as the Kelvin’s displacement fundamental solutions [27,28], i.e.,

$$U_{ij} = \begin{cases} A\{-B\delta_{ij}\ln(r)+r_{,i}r_{,j}\} & 2D \\ \frac{A}{r} \{B\delta_{ij}+r_{,i}r_{,j}\} & 3D \end{cases} \quad (26)$$

where

$$A = \frac{1}{8\alpha\pi(1-\nu)}, \quad B = 3-4\nu \quad (27)$$

with ν in Eq. (27) being a reference value of Poisson’s ratio, which can be taken as the average value of all the Poisson’s ratios of the anisotropic problem under consideration. The related kernel functions appearing in Eqs. (20) and (24) can be derived as follows

$$U_{ik,l} = \frac{-A}{r^\alpha} \{B\delta_{ik}r_{,l}-\delta_{il}r_{,k}-\delta_{kl}r_{,i}+\beta r_{,i}r_{,k}r_{,l}\} \quad (28)$$

$$U_{ij,kl} = \frac{A}{r^\beta} \{ \delta_{il}\delta_{jk} + \delta_{ik}\delta_{jl} - B\delta_{ij}\delta_{kl} - \beta(\delta_{ik}r_{,j}r_{,l} + \delta_{jk}r_{,i}r_{,l} - B\delta_{ij}r_{,k}r_{,l} + \delta_{jl}r_{,i}r_{,k} + \delta_{kl}r_{,i}r_{,j} + \delta_{il}r_{,j}r_{,k}) + \beta\gamma r_{,i}r_{,j}r_{,k}r_{,l} \} \quad (29)$$

where $\beta=2$ for 2D and $\beta=3$ for 3D problems; $\alpha=\beta-1$; $\gamma=\beta+2$.

For an internal point, Γ_ε in Eq. (23) is either a circle (2D) or a sphere (3D), and it is easy to integrate to obtain

$$\int_{\Gamma_\varepsilon} U_{ik,l}n_s d\Gamma = -(c\delta_{ik}\delta_{ls} + d\delta_{il}\delta_{ks} + d\delta_{is}\delta_{kl}) \quad (30)$$

where

$$c = A[a(3-4\nu)+b\beta], \quad d = A[b\beta-a] = \frac{-1}{2\beta\gamma(1-\nu)} \quad (31)$$

$$a = \frac{(1+\beta)\pi}{3}, \quad b = \frac{4\pi}{18-\beta} \quad (32)$$

Substituting Eqs. (30)–(32) into Eq. (23) results in

$$\mu_{ij} = \frac{1}{2\beta\chi} [2(\chi-1)D_{isjs}-D_{ijss}] \quad (33)$$

where

$$\chi = \gamma(1-\nu) \quad (34)$$

From Eq. (33), it can be seen that the coefficient μ_{ij} is a symmetric tensor, i.e., $\mu_{ij} = \mu_{ji}$.

Eq. (33) is an expression for general anisotropic elasticity problems. For an isotropic material, $D_{ijkl} = \lambda\delta_{ij}\delta_{kl} + \mu(\delta_{ik}\delta_{jl} + \delta_{il}\delta_{jk})$, with μ being the shear modulus. It is easy to prove that $\mu_{ij} = \mu\delta_{ij}$,

$U_{ik,ls}D_{kljs} = 0$, and, in this case, Eqs. (24) and (25) are reduced to the results in [16,30].

4. Transformation of domain integrals into boundary integrals

The domain integrals involved in Eqs. (9) and (25) can be evaluated using the standard cell-discretization technique [28]. However, this will remove the distinct advantage of BEM of requiring only that the boundary of the problem needs to be discretized into elements. To retain this advantage, the radial integration method (RIM) [21,22] is adopted in this paper to transform all the domain integrals included in Eqs. (9) and (25) into equivalent boundary integrals.

In terms of RIM, a domain integral with integrand $f(\mathbf{x},\mathbf{y})$ can be transformed into an equivalent boundary integral as follows:

$$\int_{\Omega} f(\mathbf{x},\mathbf{y})d\Omega(\mathbf{x}) = \int_{\Gamma} \frac{1}{r^\alpha} \frac{\partial r}{\partial n} F(\mathbf{z},\mathbf{y})d\Gamma(\mathbf{z}) \quad (35)$$

where $\alpha=1$ for 2D and $\alpha=2$ for 3D domain integrals, $r(\mathbf{z},\mathbf{y})$ denotes the distance between points \mathbf{y} and \mathbf{z} , and $F(\mathbf{z},\mathbf{y})$ is determined by the following radial integral

$$F(\mathbf{z},\mathbf{y}) = \int_0^{r(\mathbf{z},\mathbf{y})} f(\mathbf{x},\mathbf{y})r^\alpha dr \quad (36)$$

To evaluate the radial integral (36), the coordinates \mathbf{x} in $f(\mathbf{x},\mathbf{y})$ need to be expressed in terms of the integration variable r using the following relationship

$$x_i = y_i + r_{,i}r \quad (37)$$

in which the quantities y_i and $r_{,i}$ are constant in the radial integral (36).

For some simple functions, Eq. (36) can be analytically integrated. However, for complicated functions, Gaussian quadrature may be used to numerically evaluate Eq. (36) [21,22]. The domain integrals caused by source Q or body force b_j in Eqs. (9) and (25) can be directly and accurately transformed into boundary integrals using RIM formulations (35) and (36) [21], since Q and b_j are usually known functions. However, for the first domain integrals involved in Eqs. (9) and (25), the radial integral (36) cannot be directly evaluated, since the unknown field variables T and u_j are included in the resulting integrands. Therefore, to use RIM, T and u_j are approximated in this study by a series of prescribed basis functions, usually by radial basis functions (RBFs) [16,26,30,31]. In this approximation, the potential T can be expressed as

$$T(\mathbf{x}) = \sum_A \alpha^A \phi^A(R/S_A) + a^j x_j + a^0 \quad (38a)$$

$$\sum_A \alpha^A = \sum_A \alpha^A x_j^A = 0 \quad (38b)$$

where $R = \|\mathbf{x}-\mathbf{x}^A\|$ is the distance from the application point \mathbf{x}^A to the field point \mathbf{x} , S_A is the size of the support region for RBFs at point \mathbf{x}^A , and α^A and a^k are coefficients to be determined. Investigations show that the 4th order spline RBF can give very stable results [30], which can be expressed as

$$\phi^A(R/R_A) = \begin{cases} 1-6\left(\frac{R}{S_A}\right)^2 + 8\left(\frac{R}{S_A}\right)^3 - 3\left(\frac{R}{S_A}\right)^4 & 0 \leq R \leq S_A \\ 0 & R \geq S_A \end{cases} \quad (39)$$

In this study, the support size S_A is determined by specifying the number of application points around \mathbf{x}^A , while the coefficients α^A and a^k are determined by collocating \mathbf{x} in Eq. (38) at all application points. As a result, a set of algebraic equations can be

obtained in the following matrix form

$$\{T\} = [\phi]\{\alpha\} \tag{40}$$

where $\{T\}$ is a vector of the potential at all application points, and $\{\alpha\}$ is a vector consisting of the coefficients α^A for all application points and a^k . If there are no two points having the same coordinates, the matrix $[\phi]$ is invertible and thereby

$$\{\alpha\} = [\phi]^{-1}\{T\} \tag{41}$$

Similarly, u_i can be approximated using an RBF as

$$u_i = \sum_A \alpha_i^A \phi^A(R/S_A) + a_i^j x_j + a_i^q \tag{42a}$$

$$\sum_A \alpha_i^A = \sum_A \alpha_i^A x_j^A = 0 \tag{42b}$$

and coefficients α_i^A and a_i^k are determined using

$$\{\alpha_i\} = [\phi]^{-1}\{u_i\} \tag{43}$$

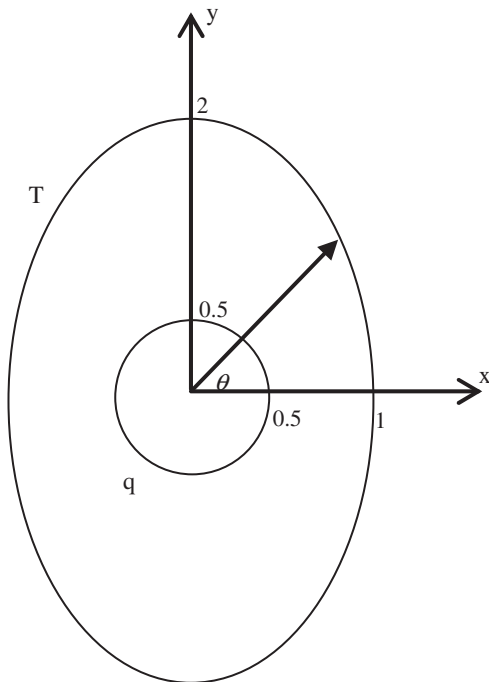


Fig. 2. Geometry and boundary conditions for the hollow ellipse.

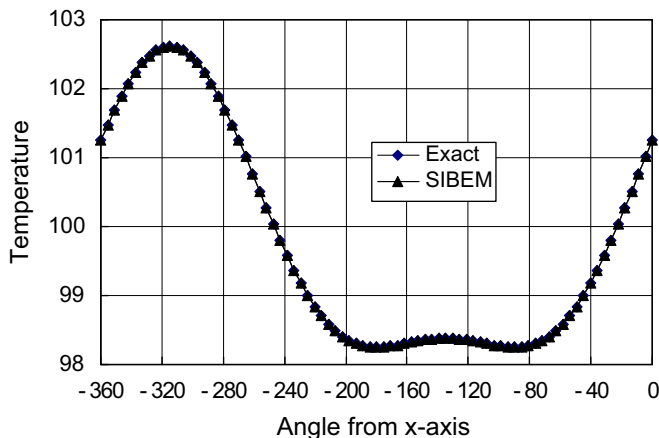


Fig. 3. Distribution of temperature over inner boundary.

where $\{u_i\}$ is a vector consisting of the i -th components of all nodal displacements.

After approximating the potential and displacement using Eqs. (38) and (42), the first domain integrals in Eqs. (9) and (25) can be transformed into boundary integrals using RIM formulations (35)–(37). The transformation procedure is the same as those described in [26,16,30]. The reader is encouraged to refer to these references for further details.

5. Numerical examples

A Fortran code called an SIBEM has been developed using the formulations presented in this paper based on the use of isotropic fundamental solutions. The code is based on a modification of the source code BEMECH given in [28]. In view of the fact that general practical engineering problems are usually composed of different materials or sub-structures, the three-step multi-domain BEM solver developed in [32] is built in an SIBEM. The three-step MDBEM solver was particularly developed for solving nonhomogenous and nonlinear problems. One of its features is that large-scale problems can be solved efficiently. To handle structural multiscale problems, in which the size in one direction is much smaller than those in other directions, an unequally spaced element sub-division technique is used in an SIBEM based on the integration strategy of the equally

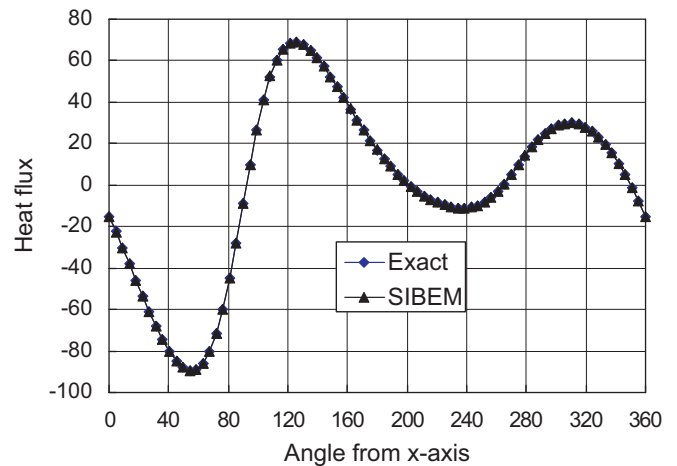


Fig. 4. Distribution of heat flux over outer boundary.

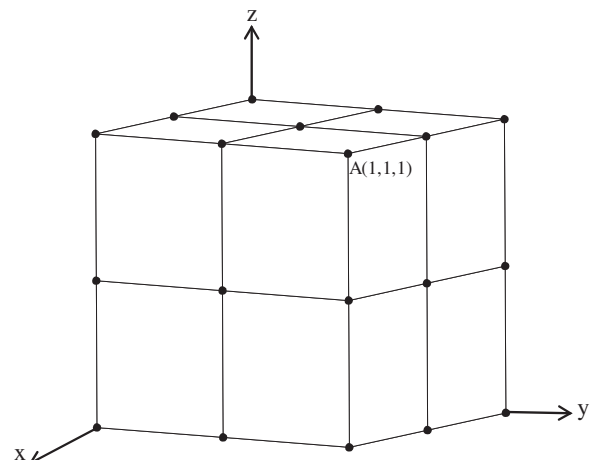


Fig. 5. Anisotropic cube in uniform tension.

spaced element sub-division technique described in [28] for evaluating nearly singular integrals. This technique is very efficient for solving thin or narrow structural problems. To model the feature of multiple values of the flux and traction at corner and edge points, the discontinuous element technique [32,27] is used in an SIBEM. To verify the correctness and capabilities of the developed code SIBEM, a 2D anisotropic heat conduction problem and three 3D transversely isotropic elastic problems are analyzed in the following examples.

5.1. Heat conduction over an anisotropic hollow ellipse

The first example is concerned with the heat conduction over a hollow ellipse with dimensions as shown in Fig. 2. The varying heat conductivity k_{ij} is specified as

$$[k] = \begin{bmatrix} x+y+5 & 1 \\ 1 & x+y+4 \end{bmatrix}$$

The temperature satisfying the governing Eq. (1) without a heat generator is [25]

$$T(x,y) = -x^2 - y^2 + 6xy + 3x + 3y + 100$$

Table 1 Displacement for anisotropic cube in uniform tension.

	Exact solution ($\times 10^{-6}$ m)	SIBEM ($\times 10^{-6}$ m)	Load direction
u_x	4.673	4.6730	x
u_y	-1.242	-1.2420	
u_z	-0.948	-9.4806	
u_x	-1.242	-1.2420	y
u_y	7.162	7.1626	
u_z	-1.387	-1.3878	
u_x	-0.948	-9.4806	z
u_y	-1.387	-1.3878	
u_z	7.252	7.2526	

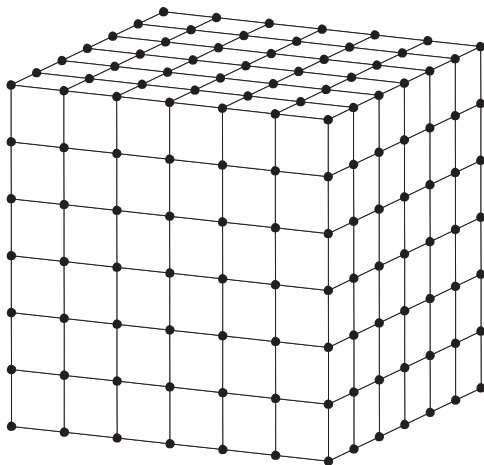


Fig. 6. BEM model of the varying coefficient cube.

Table 2 Displacements for anisotropic FGM cube ($\times 10^{-6}$ m).

No. of internal points	0	1	8	27	64	125	216
u_x	-0.4409	-0.7386	-0.1002	-0.3030	-0.2743	-0.3174	-0.3261
u_y	-1.4324	-1.4517	-1.0819	-1.0153	-0.9159	-0.9427	-1.0126
u_z	3.7125	4.5289	2.5884	3.4846	3.5126	3.5677	3.5363

The boundary conditions (B.C.) are specified by the temperature on the outer elliptical boundary and the heat flux on the inner circular boundary, which are computed using the above temperature function. The boundary of the hollow ellipse is discretized into eighty quadratic boundary elements. No internal points are used. Fig. 3 gives the variation of the computed temperature versus the angle θ (see Fig. 2) over the inner circular boundary, in which fluxes are specified as B.C. Fig. 4 shows the case of the computed flux over the outer elliptical boundary over which temperatures are specified. Figs. 3 and 4 show that the SIBEM results are in excellent agreement with the exact solutions. This indicates that even without the use of any internal points, SIBEM can still give very satisfactory results due to the use of RIM [21,22] in the transformation of the domain integrals included in Eq. (9) to the boundary integrals.

5.2. Transversely isotropic elastic cube in uniform tension

The second example deals with a cube with dimensions of $1 \times 1 \times 1$ m³ subject to a uniform tension load. The following transversely isotropic material properties [17] are used, in which the unit is 10⁴ Mpa.

$$[D] = \begin{bmatrix} 23.5 & 4.85 & 4. & 0. & 0. & 0. \\ & 15.5 & 3.6 & 0. & 0. & 0. \\ & & 15.0 & 0. & 0. & 0. \\ & & & 12. & 0. & 0. \\ & & & & 1.4 & 0. \\ & & & & & 7. \end{bmatrix}$$

Symmetric

The elastic constitutive equation corresponding to the above material matrix is $\{\sigma\} = [D]\{\varepsilon\}$, where $\{\sigma\}^T = \{\sigma_{11}, \sigma_{22}, \sigma_{33}, \sigma_{12}, \sigma_{23}, \sigma_{31}\}$ and $\{\varepsilon\}^T = \{\varepsilon_{11}, \varepsilon_{22}, \varepsilon_{33}, \varepsilon_{12}, \varepsilon_{23}, \varepsilon_{31}\}$. Six surfaces of the cube are discretized into 26 linear boundary elements (Fig. 5) and no internal points are defined. The three surfaces corresponding to $x=0, y=0,$ and $z=0$ are imposed with roller boundary conditions, i.e. the normal displacement and tangential tractions are zero.

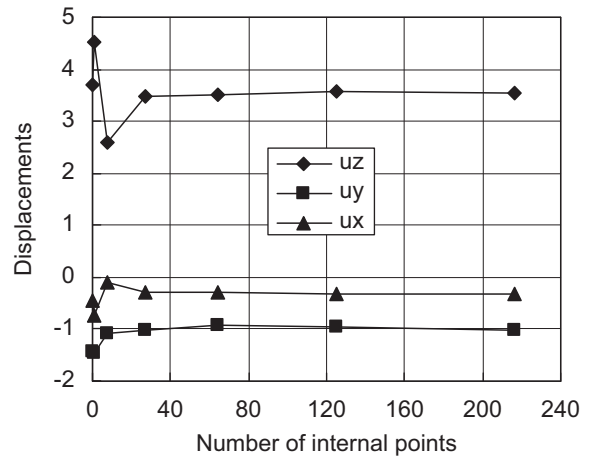


Fig. 7. Variation of displacements versus number of internal points.

Three load cases are considered by imposing a unit tension of 1 kN/m^2 over three surfaces with normal directions along the three axes. An exact solution exists for this problem [6]. Table 1 lists the computed displacements for point A (see Fig. 5) using an SIBEM and the exact solution. It can be seen that the results of SIBEM are very close to the exact solutions. This demonstrates that the formulations presented in the paper are correct.

5.3. Transversely isotropic elastic cube with varying material properties

The third numerical example considers the same problem setup as described in the second example, but the material is functionally graded in the x -direction in such a way that all elements in the matrix $[D]$ listed in example two vary following

the same rule that $[D]_{FGM} = [D]e^{\alpha x}$ with $\alpha = 1.61$. This means that the value of the elasticity matrix at $x=1$ is five times that at $x=0$.

Here, we only consider the load case of $t_z = 1 \text{ kN/m}^2$, which is imposed on the top surface of the cube. Since the stiffness matrix $[D]_{FGM}$ varies nonlinearly, more elements are required than in the second example. The six surfaces of the cube are discretized into 216 linear boundary elements with 218 boundary nodes (Fig. 6).

To ensure computational accuracy, equally spaced internal points are defined in the cube. To examine the dependence of the results on the number of internal points, different computations are carried out using different numbers of internal points. Table 2 gives the computed displacements at point A (see Figs. 5 and 7) is a plot of the results.

From Fig. 7, we can see that internal points are necessary for varying coefficient anisotropic problems to ensure computational accuracy. However, only 27 internal points are sufficient in this example to obtain a modest result.

5.4. Honeycomb sandwich structure with isotropic and transversely isotropic material properties

To demonstrate the ability of the proposed technique to solve challenging complex 3D geometry problems, a honeycomb sandwich structure is analyzed in this fourth example. The structure consists of upper and lower facesheets with thicknesses

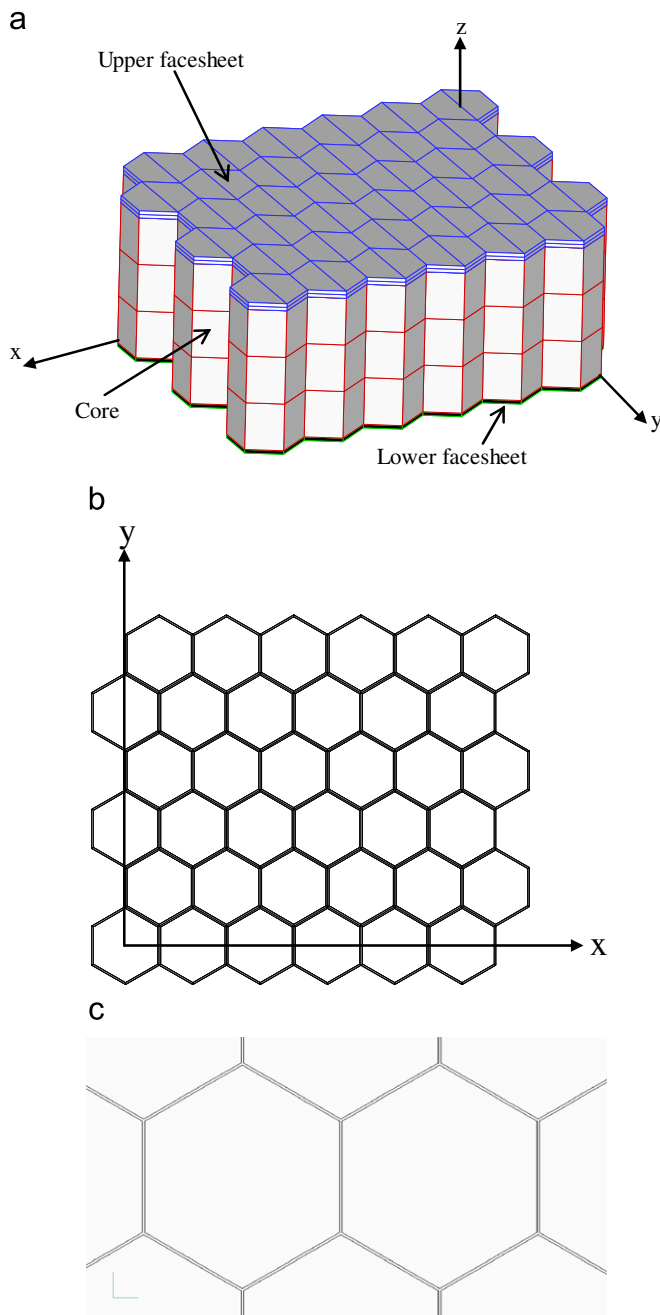


Fig. 8. BEM model for the honeycomb sandwich structure. (a) global model; (b) top view of the core; (c) enlarged top view of the core.

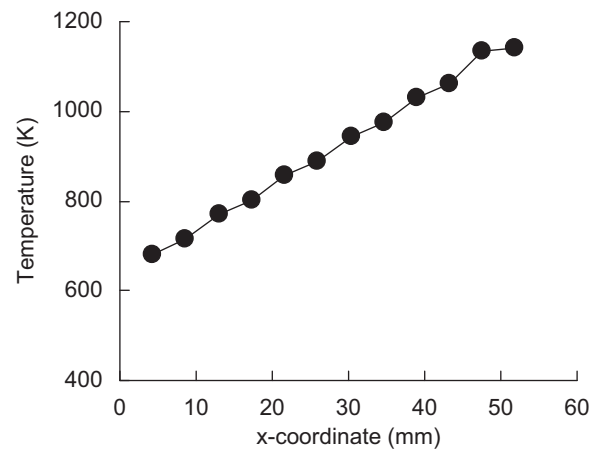


Fig. 9. Variation of temperature.

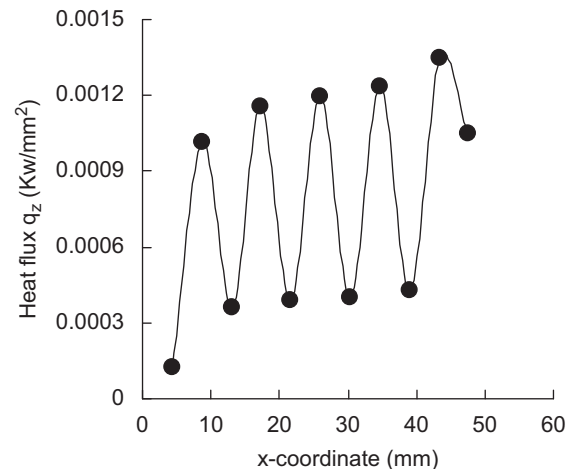


Fig. 10. Heat flux, q_z , along x -direction over wall and cavum of the honeycomb.

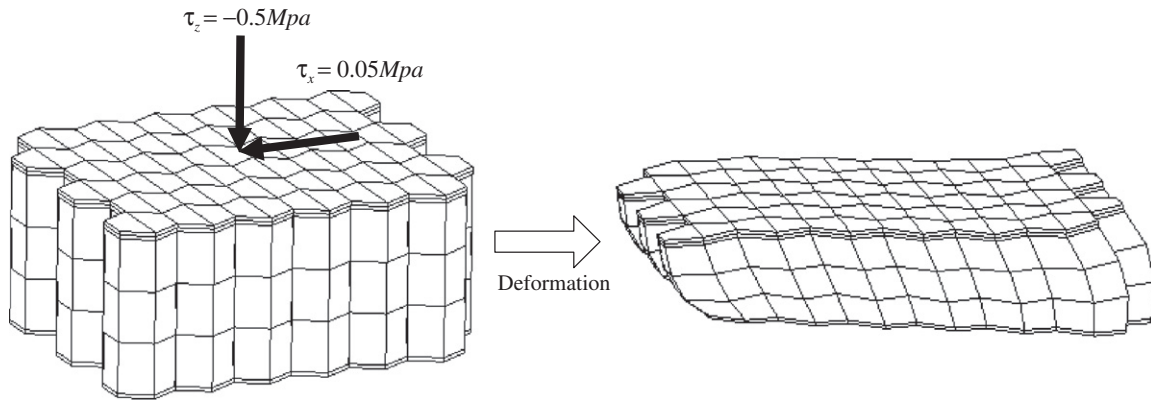


Fig. 11. Deformed mesh of the honeycomb.

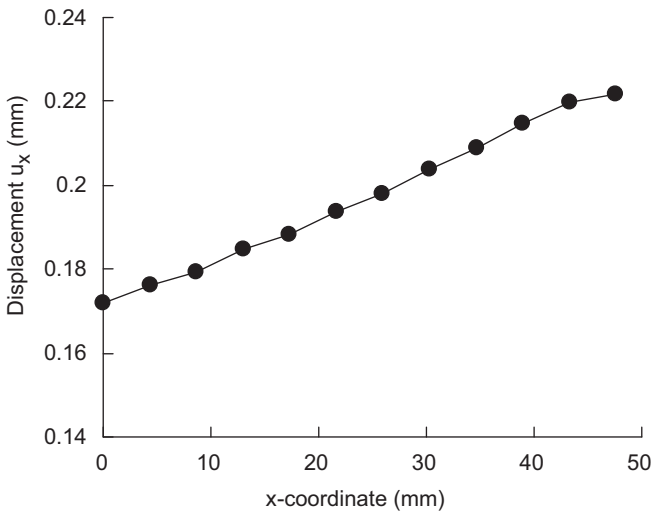


Fig. 12. Distribution of displacement u_x in the x direction.

of 1 and 0.5 mm, respectively, and the honeycomb core with dimensions of the wall thickness being 0.2 mm, wall height being 20 mm, and width of each side of the six walls being 5 mm. The structure has a total of 66 honeycombs with global dimensions of $56.1188 \times 47.5 \times 21.5 \text{ mm}^3$.

Fig. 8 shows the BEM model consisting of 2868 four-noded boundary and interface elements with 3804 boundary nodes. The upper and lower facesheets, honeycomb wall, and hollow volume are treated as different sub-domains.

5.4.1. Heat conduction computation for transversely isotropic medium

In this computation, we simulate a real thermal protection system [33] of an aircraft with the geometry structure as shown in Fig. 8. The upper facesheet is considered as a thermal isolation lid consisting of a fibrous material with transversely isotropic properties of $k_{11} = k_{22} = 7.8 \times 10^{-5} \text{ W}/(\text{mm} \cdot \text{K})$, $k_{33} = 3.0 \times 10^{-5} \text{ W}/(\text{mm} \cdot \text{K})$, and other $k_{ij} = 0$ for $i \neq j$. The conductivities are $7.8 \times 10^{-5} \text{ W}/(\text{mm} \cdot \text{K})$ for the lower facesheet, $1.7 \times 10^{-4} \text{ W}/(\text{mm} \cdot \text{K})$ for the honeycomb wall, and $2.3 \times 10^{-5} \text{ W}/(\text{mm} \cdot \text{K})$ for the filled air in the hollow volume of the core. The thermal boundary conditions are as follows: the top and bottom surfaces are specified with the temperature computed using $T(x,y,z) = 10x + 10y + 10z + 200$ (K) and the side surfaces are adiabatic. Figs. 9 and 10 are computed temperature and heat flux over the line of ($z = 19.9 \text{ mm}, y = 22.5 \text{ mm}$). In Fig. 10, the points

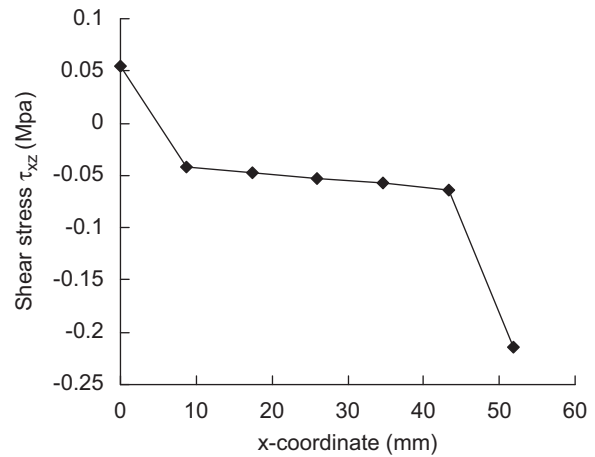


Fig. 13. Shear stress σ_{xz} along the x -direction.

corresponding to the lower position are above the center of each honeycomb, and those corresponding to the upper position are above the honeycomb wall. Fig. 10 clearly shows that the heat flux is much larger through the honeycomb wall than through the hollow volume. This phenomenon is difficult to capture with an FEM, since the honeycomb wall is too thin to be discretized into elements in an FEM analysis.

5.4.2. Elasticity computation for transversely isotropic medium

In the following, the elasticity analysis is performed for the honeycomb sandwich structure described above. The top surface is uniformly imposed with traction conditions of $\tau_x = 0.05 \text{ Mpa}$ and $\tau_z = -0.5 \text{ Mpa}$, the bottom surface is fixed, and the side surface is traction-free. The material parameters are taken as follows for the upper facesheet

$$[D_{top}] = \begin{bmatrix} 160. & 108. & 106. & 0. & 0. & 0. \\ & 160. & 106. & 0. & 0. & 0. \\ & & 248. & 0. & 0. & 0. \\ & & & 72. & 0. & 0. \\ \text{Symmetric} & & & & 104. & 0. \\ & & & & & 104. \end{bmatrix}$$

The sandwich core and lower sheet are treated as isotropic materials, both having Young's modulus of $E = 280 \text{ Gpa}$. The sub-domain of the hollow volumes is not considered in the elasticity computation and the corresponding surfaces are imposed with traction-free boundary conditions. The Poisson's ratio $\nu = 0.25$ is used for all sub-domains.

Fig. 11 shows the original and deformed meshes drawn using computed displacements enlarged 80 times, and Figs. 12 and 13 give the computed horizontal displacement along the line of ($z=20.1, y=20$) and the shear stress σ_{xz} along the line of ($y=20, z=-0.5$) on the bottom surface, respectively. Although no existing analytical or numerical results can be used to verify the computed results, the distribution trends of the displacements and stresses are correct.

6. Conclusions and discussion

In this paper, a simple but robust boundary element method is presented based on a source point isolation technique. Mathematically, the technique is stemmed from the Cauchy principal value concept. Nevertheless, the term of “source point” is commonly used in BEM. Therefore, the proposed method is called the Source-point Isolation Boundary Element Method (SIBEM). The derived boundary-domain integral equations can be used to solve anisotropic, nonlinear potential and elasticity problems. For nonlinear problems, the material property matrices k_{ij} and D_{klrs} may be the functions of field quantities such as temperatures and/or stresses. In this case, an iterative procedure is required to solve the resulting system of equations [29].

Different types of fundamental solutions can be used for a specific problem, although isotropic fundamental solutions are adopted in the paper, which result in simple and explicit integral equations. Fundamental solutions with singularities of Green's functions are preferable, since this type of solutions can result in finite values of the free term coefficients appearing in the boundary-domain integrals, as shown in Eqs. (15) and (33).

The domain integrals involved in the integral equations are transformed into boundary integrals using an RIM and, consequently, internal cell discretization is avoided. Numerical examples show that accurate computational results can be achieved using the presented SIBEM and few internal points are required to obtain a satisfactory result.

Acknowledgement

The author gratefully acknowledges the National Natural Science Foundation of China for financial support to this work under Grant NSFC no. 10872050.

References

- [1] Chen JT, Hong HK. Review of dual boundary element methods with emphasis on hypersingular integrals and divergent series. *Appl Mech Rev ASME* 1999;52(1):17–33.
- [2] Lie Kyoong-Haeng Choh, Koehler JS. The elastic stress field produced by a point force in a cubic crystal. *Adv Phys* 1968;17:421–78.
- [3] Pan YC, Chou TW. Point force solution for an infinite transversely isotropic solid. *Trans ASME, J Appl Mech* 1976;608–12.
- [4] Barnett DM. The precise evaluation of derivatives of the anisotropic elastic Green's functions. *Phys Status Solidi (b)* 1978;49:741–8.
- [5] Mura T. *Micromechanics of defects in solids*. 2nd ed.. Dordrecht, The Netherlands: Martinus Nijho; 1987.
- [6] Lekhnitskii SG. *Theory of elasticity of an anisotropic body*. Moscow: Mir Publishers; 1981.
- [7] Sollero P. *Fracture mechanics analysis of anisotropic laminates by the boundary element method*. Ph.D. Thesis, Wessex Institute of Technology; 1994.
- [8] Comino L, Marin L, Gallego R. An alternating iterative algorithm for the Cauchy problem in anisotropic elasticity. *Eng Anal Boundary Elem* 2007;31:667–82.
- [9] Shiah YC, Tan CL. Calculation of interior point stresses in two-dimensional boundary element analysis of anisotropic bodies with body forces. *J Strain Anal Eng Des* 1999;34:117–28.
- [10] Wang CY. Elastic fields produced by a point source in solids of general anisotropy. *J Eng Math* 1997;32:41–52.
- [11] Toton F, Amadei B. Green's functions and boundary element method formulation for 3D anisotropic media. *Comput Struct* 2001;79:469–82.
- [12] Ting TCT, Lee VG. The three-dimensional elastostatic Green's function for general anisotropic linear elastic solids. *Q J Mech Appl Math* 1997;50:407–26.
- [13] Stroh AN. Steady state problems in anisotropic elasticity. *J Math Phys* 1962;41:77–103.
- [14] Fares N, Li VC. General image method in a plane-layered elastostatic medium. *J Appl Mech* 1988;55:781–5.
- [15] Pan E, Yuan FG. Three-dimensional Green's functions in anisotropic bimetals. *Int J Solids Struct* 2000;37:5329–51.
- [16] Gao XW, Ch Zhang, Sladek J, Sladek V. Fracture analysis of functionally graded materials by a BEM. *Compos Sci Technol* 2008;68:1209–15.
- [17] Schlar NA, Partridge PW. 3D anisotropic elasticity with BEM using the isotropic fundamental solution. *Eng Anal Boundary Elem* 1993;11:137–44.
- [18] Nardini D, Brebbia CA. A new approach for free vibration analysis using boundary elements. In: Brebbia CA, editor. *Boundary element methods in engineering*. Berlin: Springer; 1982. p. 312–26.
- [19] Chen CS, Marozzi M, Choi S. The method of fundamental solutions and compactly supported radial basis functions—a meshless approach to 3D problems. In: Brebbia CA, Power H, editors. *Boundary Element Methods XXI*. Boston/Southampton: WIT Press; 1999. p. 561–70.
- [20] Chen CS, Rashed YF, Golberg MA. A mesh-free method for linear diffusion equations. *Numer Heat Transfer Part B* 1998;33:469–86.
- [21] Gao XW. The radial integration method for evaluation of domain integrals with boundary-only discretization. *Eng Anal Boundary Elem* 2002;26:905–16.
- [22] Gao XW. A boundary element method without internal cells for two-dimensional and three-dimensional elastoplastic problems. *ASME J Appl Mech* 2002;69:154–60.
- [23] Albuquerque EL, Sollero P, Paiva WP. The radial integration method applied to dynamic problems of anisotropic plates. *Commun Numer Meth Eng* 2007;23:805–18.
- [24] Hematiyan MR. A general method for evaluation of 2D and 3D domain integrals without domain discretization and its application in BEM. *Comput Mech* 2007;39(4):509–20.
- [25] Divo EA, Kassab AJ. *Boundary element methods for heat conduction: with applications in non-homogeneous media*. Southampton: WIT Press; 2003.
- [26] Gao XW. A meshless BEM for isotropic heat conduction problems with heat generation and spatially varying conductivity. *Int J Numer Meth Eng* 2006;66:1411–31.
- [27] Brebbia CA, Dominguez J. *Boundary elements: an introductory course*. London: McGraw-Hill Book Co.; 1992.
- [28] Gao XW, Davies TG. *Boundary element programming in mechanics*. Cambridge, UK: Cambridge University Press; 2002.
- [29] Gao XW, Ch Zhang. Isotropic damage analysis of elastic solids using meshless BEM. *Key Eng Mater* 2006;324–5. 1261–1264.
- [30] Gao XW, Ch Zhang, Guo L. Boundary-only element solutions of 2D and 3D nonlinear and nonhomogeneous elastic problems. *Eng Anal Boundary Elem* 2007;31:974–82.
- [31] Golberg MA, Chen CS, Bowman H. Some recent results and proposals for the use of radial basis functions in the BEM. *Eng Anal Boundary Elem* 1999;23:285–96.
- [32] Gao XW, Guo L, Zhang Ch. Three-step multi-domain BEM solver for nonhomogeneous material problems. *Eng Anal Boundary Elem* 2007;31:965–73.
- [33] Blosser ML, et al. Advanced metallic thermal protection system development, *AIAA* 2002-0504, p. 1–20.